EFFECTS OF Sr-SUBSTITUTION ON THE MICROSTRUCTURE AND MAGNETIC BEHAVIOR OF M-TYPE HEXAGONAL FERRITES SYNTHESIS BY CO-PRECIPITATION METHOD

M. I. ARSHAD[a], N. AMIN[a], M. U. ISLAM[b], A. ALI[a], K. MAHMOOD[a],
M. E. UN NABI[a], M. S. AWAN[c], H. ANWAR[d], M. R. SALEEM[a],
G. MUSTAFA[b*]

[a]*Department of Physics, G.C. University, Faisalabad 38000, Pakistan*
[b]*Department of Physics, Bahauddin Zakariya University Multan 60800, Pakistan*
[c]*ISIT, Sector H-11/4, Islamabad 44000, Pakistan*
[d]*Department of Physics, University of Agriculture Faisalabad, Pakistan*

In this work, the $Ba_{1-x} Sr_x Fe_{12} O_{19}$ hexaferrites (x = 0.0, 0.2, 0.4, 0.6, 0.8 and 1.0) were synthesized by using co-precipitation method and sintered at a temperature of 1100 ºC for 8h. The investigation of structural and magnetic properties was carried out for the samples using X-ray diffraction (XRD) and magnetometer also employed to measure the magnetic properties. XRD reveals that the structure of these nanoparticles is hexagonal phase and average crystallite sizes calculated from Debye Scherrer formula lies in the range of (27.03-74.4 nm). Lattice parameters were found to be increases linearly with Sr-concentrations. Grain size estimated from scanning electron microscopy (SEM) and found to be increase with increasing Sr^{+3} content. The elemental analysis was done by EDXS and it is close agreement with the expected composition from the stoichiometry of the reactant solutions. Magnetic measurements showed that coercivity and retentivity increases from (1.22-1.47 kOe) and (1.30 - 1.70 kGauss) that varies significantly with Sr^{+3} Content. The obtained results show that the investigated materials are potential candidates for magnetic recording media and high frequency applications.

1. Introduction

The M-type hexagonal ferrites ($Ba Fe_{12} O_{19}$) are an interesting class of ferromagnetic oxides. In M type hexagonal structure Fe^{+3} are distributed in five distinct crystallographic sites, one tetrahedral ($4f_1$), three octahedral ($2a, 12k$ and $4f_2$) and one trigonal bipyramidal ($2b$) sites. In Ba-hexaferrites, along crystallographic c-axis spins of three sites 12 k, 2b and 2a sites are aligned and parallel to each other when in the magnetically ordered state while spins of $4f_2$ and $4f_1$ sites point in the opposite direction. Understanding the effects of various diamagnetic and paramagnetic cations on the magnetic properties of Sr^{+2} substituted hexaferrites is one of the most important tasks associated with use of these nanomaterials in variety of modern technological applications [1-2]. Due to high resistivity, power and eddy current loss and decreased remarkably and consequently make the synthesized ferrite materials more suitable in high frequency device fabrications. Several techniques have been developed and effectively employed for synthesis of hexaferrites such as ceramic method [3-4] solution combustion technique [5] sol-gel auto combustion process [6-7] ball milling [8] and co-precipitation technique [9-10]. Co-precipitation is one of the simplest techniques for the preparation of hexaferrite nanomaterials. In current study, we have reported the synthesis of $Ba_{1-x}Sr_xFe_{12}O_{19}$ with (x = 0.0, 0.2, 0.4, 0.6, 0.8 and 1.0) nano-hexaferrites, prepared by co-precipitation technique. In addition to that, the influence of Sr^{+2}

---

[*]Corresponding author: ghulammustafabzu@gmail.com

concentrations on the structural and magnetic properties of $Ba_{1-x}Sr_x Fe_{12}O_{19}$ nanomaterials were investigated.

2. Materials and Methods

2.1. Samples preparation and equipments

$Ba_{1-x}Sr_x Fe_{12}O_{19}$ hexaferrite samples with (x = 0.0, 0.2, 0.4, 0.6, 0.8 and 1.0) were synthesized by chemical co-precipitation technique [11-12]. The reagents $Ba(No_3)$, $Sr(No_3)_2$, $Fe(NO_3).9H_2O$ and NaOH are of analytical grade, de-ionized water was used to make the precursor. Nitrates and salts of metals with stoichiometric composition of ($Ba_{1-x}Sr_x Fe_{12}O_{19}$) were mixed in 300 mL de-ionized water. The precipitating agent was mixed drop wise during stirring until the co-precipitation occurs. When the precipitates were formed, the solution was washed thoroughly with ethanol. The precipitates were then filtered and dried at100°C for 10 h in oven. By using a mortar and pestle, the dried powder was grinded homogenously by grinding the constituents for 1 h. The pellets were formed in the hydraulic press (Paul-Otto Weber) at a pressure of 30 KN for about 3 min. The pellets were pre-sintered in a digital electric furnace for 6 h at temperature 1000° C in an ambient atmosphere. After each heat treatment the samples were extinguished in air under to have equilibrium position of the cations. The X-ray diffraction (XRD) patterns were obtained at room temperature using powder samples by using Xpert Pro PANalytical diffractometer with Cu-Kα radiation (λ = 1.54056 Å) at 40 kV and 30 mA. Intensity data was collected by the step counting method (with a scanning speed 0.05° /s) in the 2θ range from 20° - 70°. The surface morphology and microstructure of the samples were studied by JSM-6490 JEOL scanning electron microscope (SEM).The elemental composition was determined by energy dispersive peak of the representative sample using energy dispersive X-ray spectroscopy (EDXS, Model JFC-1500 JEOL).Magnetometer was used to measure the magnetic properties with a maximum applied magnetic field.

2.2. Calculations

The structural parameters such as lattice parameters ('a' and 'c'), Unit cell Volume (V cell),Crystallite size (D) and X-ray density of $Ba_{1-x}Sr_x Fe_{12}O_{19}$M-type hexaferrites were calculated from XRD data using the following formulae [13-14].

$$Sin\theta^2 = A(h^2 + hk + k^2) + C l^2 \tag{1}$$

Where $A = \frac{\lambda^2}{3a^2}$ and $C = \frac{\lambda^2}{4c^2}$

$$V_{cell} = a^2 c Sin120^0 \tag{2}$$

$$D = \frac{k\lambda}{B_{(hkl)}cos\theta} \tag{3}$$

$$\rho_{X-ray} = \frac{Z M}{N_A V} \tag{4}$$

Where 'a' and 'c' are lattice constant, (hkl) are Miller indices, V is the unit cell volume, Z represents 2 molecules per unit cell of the hexagonal structure, N_A is the Avogadro's number (6.02×10^{23}g/mol) and M is the molecular weight of the sample. Scherer's formula ascribed by equation 3 was used to calculate the crystallite size (D) nm, where, K is the shape factor, λ is the X-ray wavelength (1.54 A) and θ is the Bragg's diffraction angle.

3. Results and discussion

3.1. Structural analysis

Fig.1shows the X-ray diffraction patterns of M-type hexaferrite $Ba_{1-x}Sr_xFe_{12}O_{19}$ (x = 0.0, 0.2, 0.4, 0.6, 0.8 and 1.0). The XRD patterns were indexed and observed d-values of all the peaks were compared with JCPDS Card (00-043-0002).The diffraction peaks at 2 values are related to the diffraction planes (105), (107), (108),(109),(118), (302), (214),(217), (2013), (228) and (402). The analysis of XRD patterns indicates that the observed peak corresponds to the M-type hexagonal phase and single diffraction peak of $\alpha\text{-}Fe_2O_3$ is also observed at 2 θ = 33.2. Different parameters such as crystallite size (D), lattice constants ('a' and 'c'), unit cell volume (V_{cell}) and X-ray density (dx) calculated from the XRD data and their values were listed in (Table 1.) The lattice parameters ('a' and 'c') and unit cell volume (V_{cell}) were calculated by applying the following equations 1 and 2 [15]:
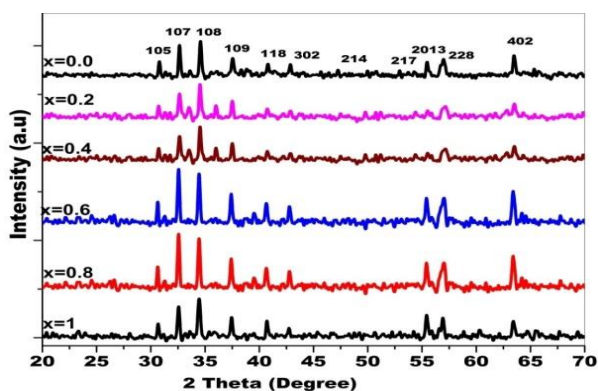

Fig.1. XRD patterns of Ba $_{1-x}$Sr$_x$ Fe$_{12}$ O $_{19}$ M-type hexaferrite powders
(x = 0.0, 0.2, 0.4, 0.6, 0.8 and 1.0) ferrites.

The lattice parameters a = (5.78 - 583Å) and c = (23.12 - 2.27Å) increase steadily with increasing the substituted amount of Sr^{2+} ions into the hexagonal lattice as shown in Fig.2.The observed variation in the lattice parameters can be explained on the basis of the relative ionic radii of Sr^{2+} = (1.32 Å) and Ba^{2+} = (1.35 Å) ions, in this case ionic radii of Ba^{2+} is larger than ionic radii Sr^{2+}, This may result in an increase in the lattice constants. The unit cell volume also increases from (668.70- 685.41 Å^3) regularly with increasing strontium content (Table 1) which may be due to increase in both the lattice parameters 'a' and 'c'. The obtained values of X-ray density listed in Table1The average crystallite size was calculated from the width of the most intense peak and was found to be in the range of (27.03 – 74.4 nm) (Table 1).
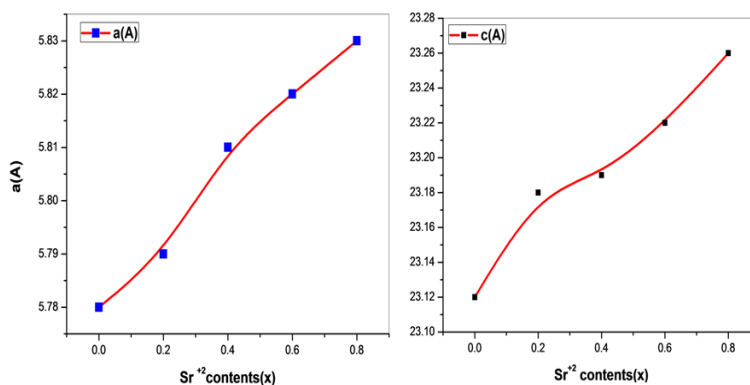

Fig.2. Variation of lattice constant 'a' and 'c' for Ba$_{1-x}$Sr$_x$ Fe$_{12}$ O $_{19}$
(x = 0.0, 0.2, 0.4, 0.6, 0.8 and 1.0) ferrites on various Sr^{+2} contents

The requirement of the grain size for high density recording media is less than 50 nm to obtain the suitable signal to noise ratio [16].The trend of the crystallite size varies by substitution strontium contents is revealed in the Fig.3
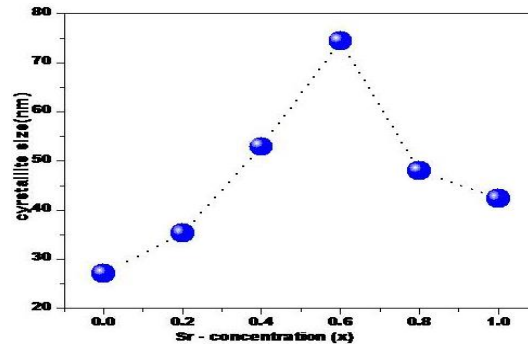

Fig.3.Crystallite size as a function of Sr^{+2} contents for Ba $_{1-x}$Sr$_x$ Fe$_{12}$ O $_{19}$
(x = 0.0, 0.2, 0.4, 0.6, 0.8 and 1.0) ferrites on various Sr^{+2} contents.

Table.1. Lattice parameters ('a' and 'c'), Unit cell Volume (V cell), Crystallite size (D),
and X-ray density of Ba $_{1-x}$Sr$_x$ Fe$_{12}$ O $_{19}$hexagonal ferrites

Composition	Lattice Parameter (a) Å	Lattice Parameter (c) Å	Unit Cell Volume ($Å^3$)	Crystallite Size (D nm)	X-ray density (g/cm^3)
Ba Fe$_{12}$ O $_{19}$	5.78	23.12	668.90	27.03	3.73
Ba $_{0.8}$Sr$_{0.2}$Fe$_{12}$ O $_{19}$	5.79	23.15	672.08	35.3	3.72
Ba $_{0.6}$Sr$_{0.4}$ Fe$_{12}$ O $_{19}$	5.80	23.18	675.75	52.9	3.74
Ba $_{0.4}$Sr$_{0.6}$Fe$_{12}$ O $_{19}$	5.81	23.24	679.84	74.4	3.73
Ba $_{0.2}$ Sr$_{0.8}$ Fe$_{12}$ O $_{19}$	5.82	23.25	682.00	48.0	3.73
Sr Fe$_{12}$ O $_{19}$	5.83	23.27	685.41	42.3	3.74

3.2. Scanning Electron Microscopy (SEM)

The SEM micrographs of the synthesized samples $Ba_{1-x}Sr_xFe_{12}O_{19}$ as a function of Sr^{+2} concentrations(x) are shown in Fig.4 (a, b, c, and d).The majorities of grains are found to be relatively well-defined hexagonal platelets and are homogeneously distributed.
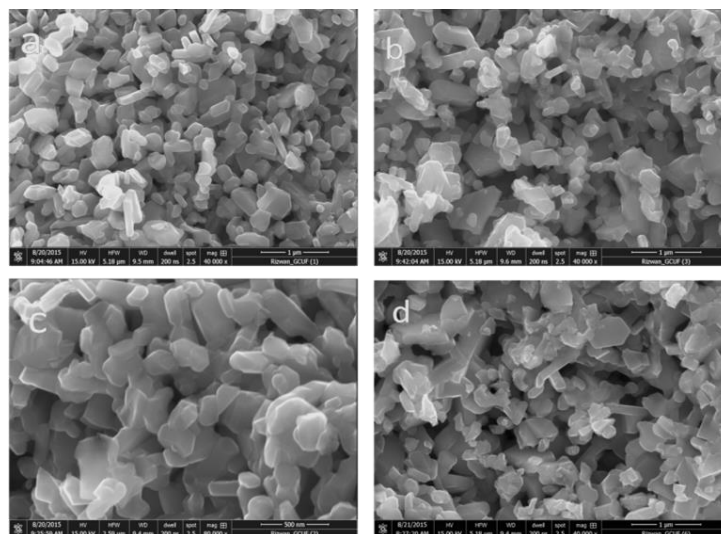

Fig.4 (a, b, c, and d) SEM images of Ba $_{1-x}$Sr$_x$ Fe$_{12}$ O $_{19}$M-type hexa ferrite

The hexagonal platelet-like shape particles with smaller aspect ratio in morphology are most suitable for applications in microwave absorption materials. Xiaogu et al. [17] and Wanga et al. [18] also reported that samples of hexagonal flake shape are beneficial for microwave absorption. In the present study, the average crystallite size as calculated from XRD by Scherer formula is smaller than the average grain size derived from SEM measurements. It means that every grain is formed by aggregation of a large number of crystallites. The shape of the materials is very important for various applications in different fields.

3.3. Energy dispersive X-ray spectroscopy (EDXS)

Figure 5 (a, b, c and d) shows the selected M-type hexaferrites composition of the synthesized samples was determined by energy dispersive X-ray spectroscopy (EDXS) analysis. It is evident from the analysis that the stoichiometric amount of Sr^{2+} increases while that Ba^{2+} content decreases indicating that strontium is being substituted at barium site. The labeled peaks in the figure clearly indicate the presence of Ba, Sr, Fe and O.
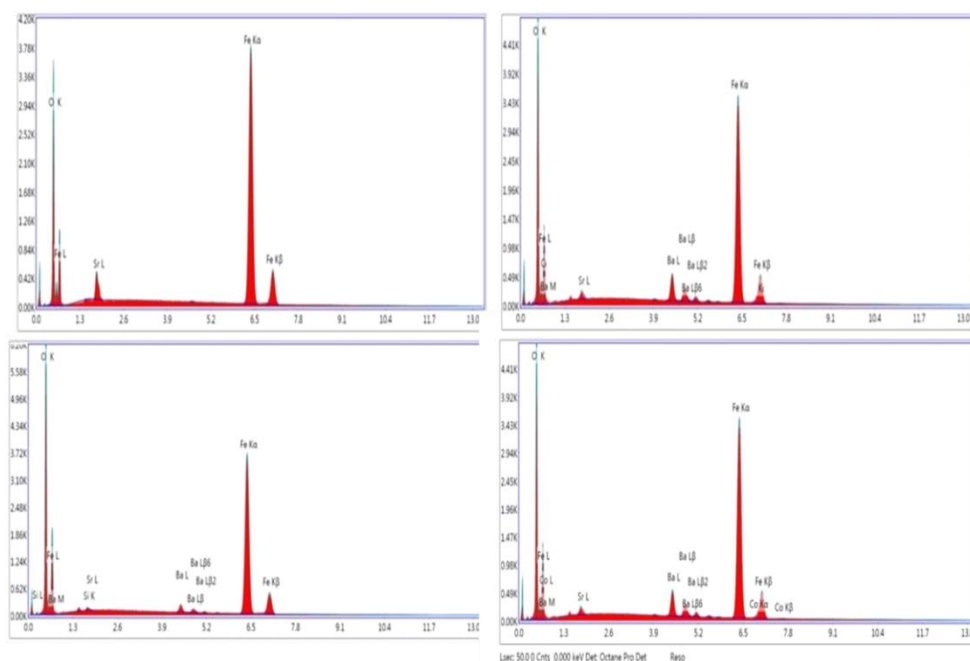

Fig. 5. EDX spectrums of $Ba_{1-x}Sr_x Fe_{12} O_{19}$ hexaferrite

3.4. Magnetic Properties

The field dependent B–H and J–H loops $Ba_{1-x}Sr_x Fe_{12} O_{19}$ (x = 0.0, 0.2, 0.4, 0.6, 0.8 and 1.0) are shows in Fig.6 (a, b, c, d and e). The upper loop represents the B–H curve and the lower loop indicates J–H curve. These hysteresis loops (B–H and J–H curves) play a very important role in comparing the magnetic properties like coercivity, loop area and retentivity by using magnetometer at room temperature. From B-H loop the magnetic parameters such as energy product (BH_{max}), coercivity (H_cB) and retentivity (Br) were measured. These magnetic parameters are strongly affected by the occupation of substituted strontium cations at different sites in the structure of hexaferrite. The values of retentivity lies in the range from ($1,307 \times 10^3$ - 1.708×10^3 Gauss) as listed in (Table 2).The retentivity is found to be enhance from (1.307×10^3 - 1.708×10^3 Gauss) with increase in Sr^{+2} contents (x). The value of retentivity is maximum for $SrFe_{12}O_{19}$ (x = 1.0) i.e. 1.708×10^3 Gauss. BH_{max}(maximum energy product) lies in the range (0.399 – 0.649 MgOe) as listed in (Table 2).The BH_{max} for unsubstituted was 0.399 MGaOe while it is highest i.e. 0.649 MGaOe for the composition $SrFe_{12}O_{19}$ (x = 1.0). HcB is found to be 1.233 kOe for the composition $BaFe_{12} O_{19}$ (x = 0.0) it increases gradually from (1.223 - 1.473 kOe) with increase in Sr^{+2} concentration(x). The enhancement in HcB was mainly due to the increase Sr^{+2} concentration and due to substitution of Sr^{+2} ions with Ba^{2+} ions. If nanomaterials have

coercively values above 1200 Oe then these can be very useful in a new developing technology of magnetic recording as perpendicular recording media [19].

Table.2. Values of magnetic parameters retentivity (B_r), coercivity (H_cB), BH_{max} and Hc (J) for different values of x in Ba $_{1-x}$Sr$_x$ Fe$_{12}$ O $_{19}$ M-type hexa ferrites.

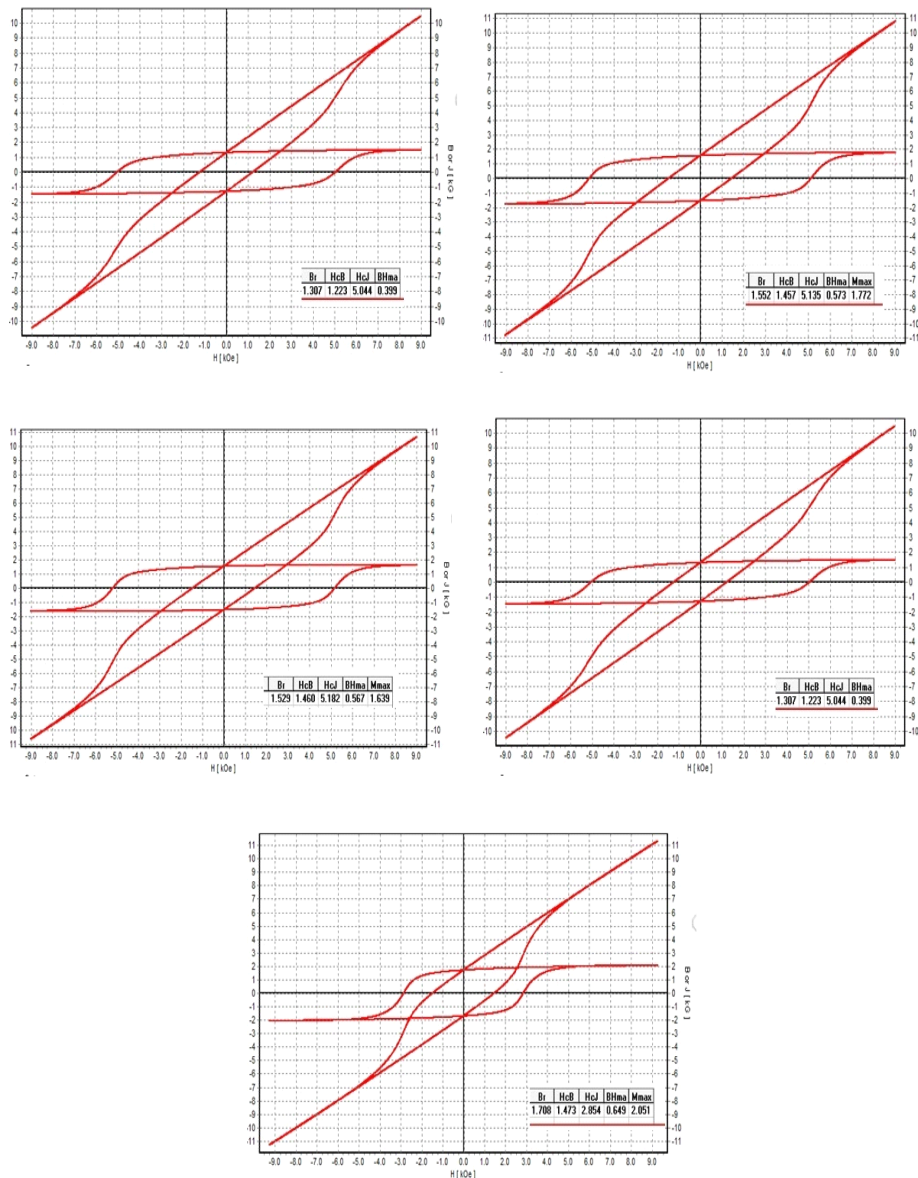| X	$B_r \times 10^3$ (Gauss)	H_cB (kOe)	$BH_{max} \times 10^{-1}$ (MGaOe)	H_cJ (kOe)
0.0	1.307	1.223	3.990	5.044
0.2	1.346	1.261	4.230	5.168
0.4	1.409	1.309	5.909	5.175
0.6	1.529	1.460	5.670	5.182
0.8	1.552	1.457	5.730	5.135
1.0	1.708	1.473	6.490	2.854

Fig.6.M-H loops of Ba $_{1-x}$Sr$_x$Fe$_{12}$O $_{19}$ hexaferrites (x=0.0, 0.2, 0.4, 0.6 and, 1.0)

Nanomaterials synthesized in the present work have coercivity H_cB values in the range (1.307 -1.708 kOe). This implies that these nanomaterials may have applications in high density magnetic recording Medias. In current study, all the synthesized nanomaterials have $H_cB > B_r/2$ (for any fixed value of Sr^{+2} ions concentration) so for high frequency applications these nanomaterials can be very beneficial as reported in the literature [20].The sample Sr $Fe_{12}O_{19}$ (x = 1.0) was found to exhibit best properties among all the synthesized samples because the magnetic parameters approached highest values as shown in (Table2). In addition to that, higher values of retentivity (B_r) and coercivity (H_cB) rendered these hexaferrite nanomaterials most beneficial for permanent magnets and for high density recording media.

4. Conclusions

Co-precipitation method effectively produced Sr^{+2} substituted hexaferrites nanocrystalline. The effect of Sr^{+3} content on the structural parameters have been studied by X-ray diffractionand found to be in hexgonal phase. The physical parameters of the material revealed that crystallite size were found in range (27.03-74.4 nm) while lattice parameters increase with the increasing of Sr^{+3} concentrations. Magnetic measurements show that the highest substituted Sr^{+2} (x = 1.0) is found to the best parameters such as energy product, retentivity (B_r) and coercivity (H_cB). These samples are useful in the magnetic recording applications, because recording media requires a high saturation magnetization and a moderately high coercivity

References

[1]H. Sozeri, J. Magn. Magn.Mater.**321**,2717 (2009).
[2] J. Lee, M. Fuger, J. Fidler, D. Suess, T. Schrefl, O. Shimizu, J. Magn. Magn.Mater. **322,** 3869 (2010).
[3] G.M. Rai, M.A. Iqbal, K.T. Kubra, J. Alloys Comp. **495**,229 (2010).
[4] M.A. Ahmed, N. Okasha, R.M. Kershi, Phys. B: Condens. Matter **405,**3223 (2010).
[5] V.N. Dhage, M.L. Mane, A.P. Keche, C.T. Birajdar, K.M. Jadhav, Phys. B:CondensMatter **406,**789 (2011).
[6] L. Junliang, Z. Yanwei, G. Cuijing, Z. Wei, Y. Xiaowei, J. Eur. Ceram. Soc. **30,** 993 (2010).
[7] M. Ahmad, Q. Ali, I. Ali, I. Ahmad, M. Azhar Khan, M.N. Akhtar, G. Murtaza, M.U.Rana, J. Alloys Comp. **580,**23 (2013).
[8] I. Bsoul, S.H. Mahmood, J. Alloys Comp. **489,**110 (2010).
[9] F. Aen, S.B. Niazi, M.U. Islam, M. Ahmad, M.U. Rana, Int.Ceram. **37,**1725 (2011).
[10] S. ManjuraHoque, C. Srivastava, V. Kumar, N. Venkatesh, H.N. Das, D.K. Saha, K. Chattopadhyay, Mater. Res. Bull. **48,**2871 (2013).
[11]P.Shepherd, K.K.Mallick, R.J.Green, J.Magn.Magn.Mater.**311**,683 (2007).
[12] A. Elahi, M. Ahmad, I. Ali, M.U. Rana, Ceram. Int. **39**,983 (2013).
[13] W.D. Townes, J.H. Fang, A.J. Perrotta, Zeitschrift fur KristallographieCrystalline Materials **125,**437 (1967).
[14] M.J. Iqbal, M.N. Ashiq, P. Hernandez-Gomez, J.M.M. Munoz, C.T.Cabrera, J.Alloys Comp. **500**,113 (2010).
[15] M.J. Iqbal, M.N. Ashiq, P. Hernandez-Gomez, J.M.M. Munoz, C.T. Cabrera, J.Alloys Comp. **500**,113 (2010).
[16]S. Che, J. Wang, Q. Chen, J. Phys.: Condens. Matter **15**,335 (2003).
[17]H. Xiaogu, Z. Jing, W. Hongzhou, Y. Shaoteng, W. Lixi, Z. Qitu, J. Rare Earths

28,940 (2010).
[18]L. Wanga, J. Songa, Q. Zhanga, X. Huanga, N. Xua, J. Alloys Comp. **481,**863 (2009).
[19]Y. Li, R. Liu, Z. Zhang, C. Xiong, Mater. Chem. Phys. **64**,256 (2000).
[20]S.Ounnunkada, P.Wintai, J.Magn, Magn.Mater.**301**,292 (2006).